



Advanced Optimization Capabilities in SU2 for the Design of a Low-Boom Flight Demonstrator

Sonic Boom Activities IV – Low Sonic Boom Flight Demonstration

AIAA Aviation 2014

Atlanta, GA

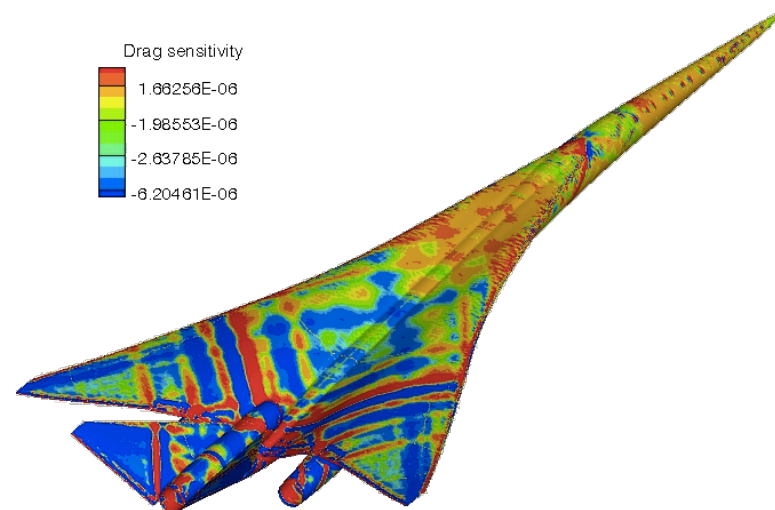
June 17, 2014

Juan J. Alonso, Francisco Palacios, Trent Lukaczyk

Department of Aeronautics & Astronautics

Stanford University

Stanford, CA 94305, U.S.A.





Outline

- The challenge of low-boom design
- Regularizing the design process
- N+2 vehicle design efforts
- Low-Boom Flight Demonstrator ongoing efforts
- Conclusions & future work



Outline

- The challenge of low-boom design
- Regularizing the design process
- N+2 vehicle design efforts
- Low-Boom Flight Demonstrator ongoing efforts
- Conclusions & future work



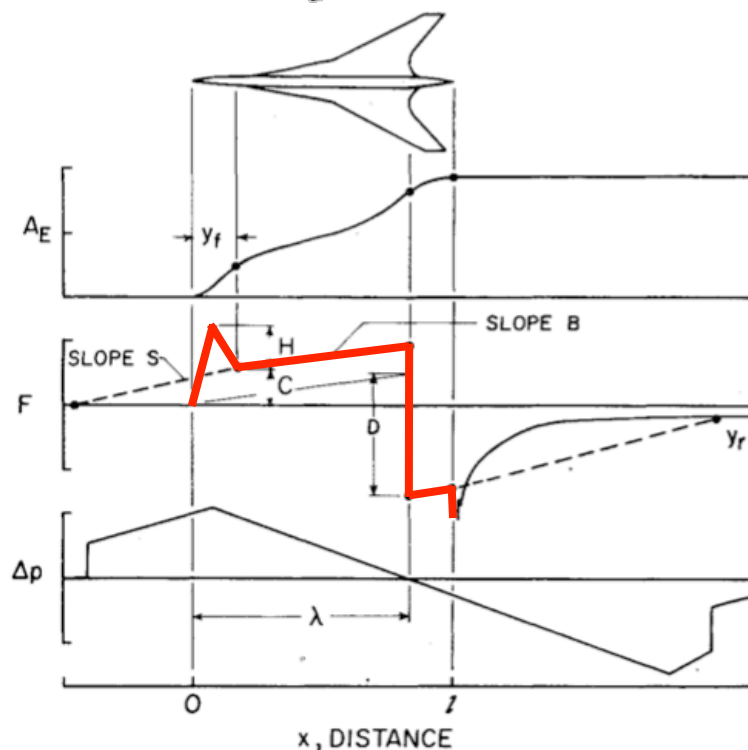
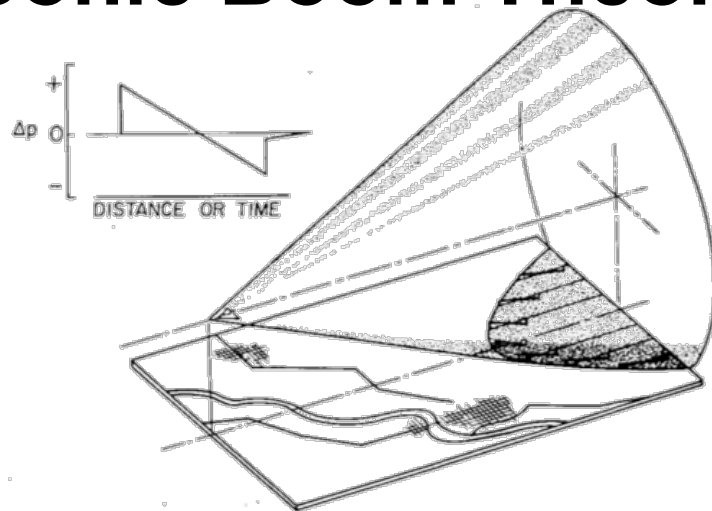
Classical Sonic Boom Theory

- Based on classical, linearized supersonic flow
- Parameterization of the F-function (near field pressure distribution) using 5 parameters
- Analytic optimization
- Drag impact of boom minimization not considered

But

- Tremendous physical insight
- Actual usable results:
 - Minimum pressure rise/overpressure/impulse
 - Target area distributions

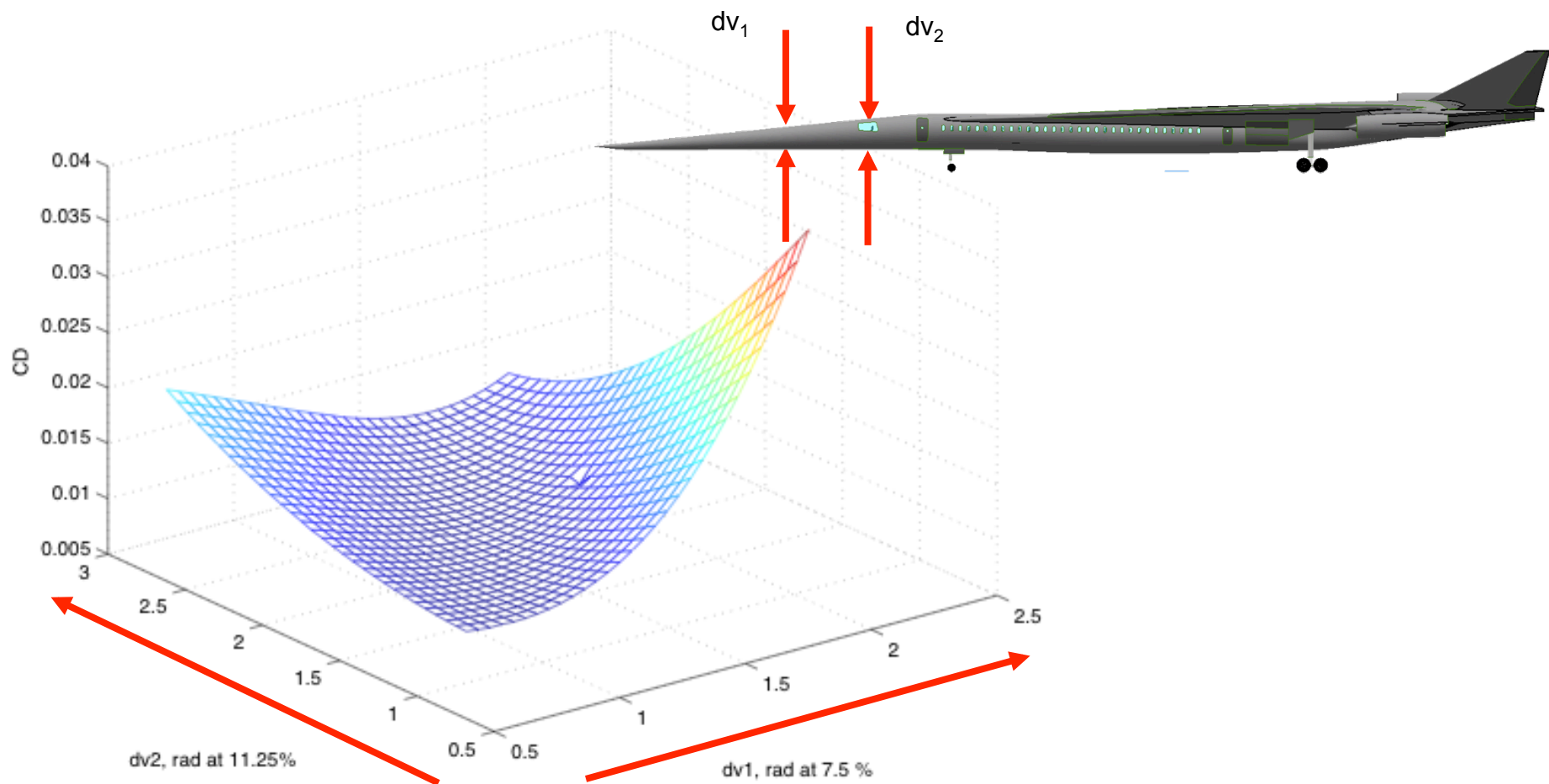
$$\Delta p \propto \frac{W_{\text{aircraft}}}{L^{3/2}}$$





Why Is Low-Boom Design Difficult?

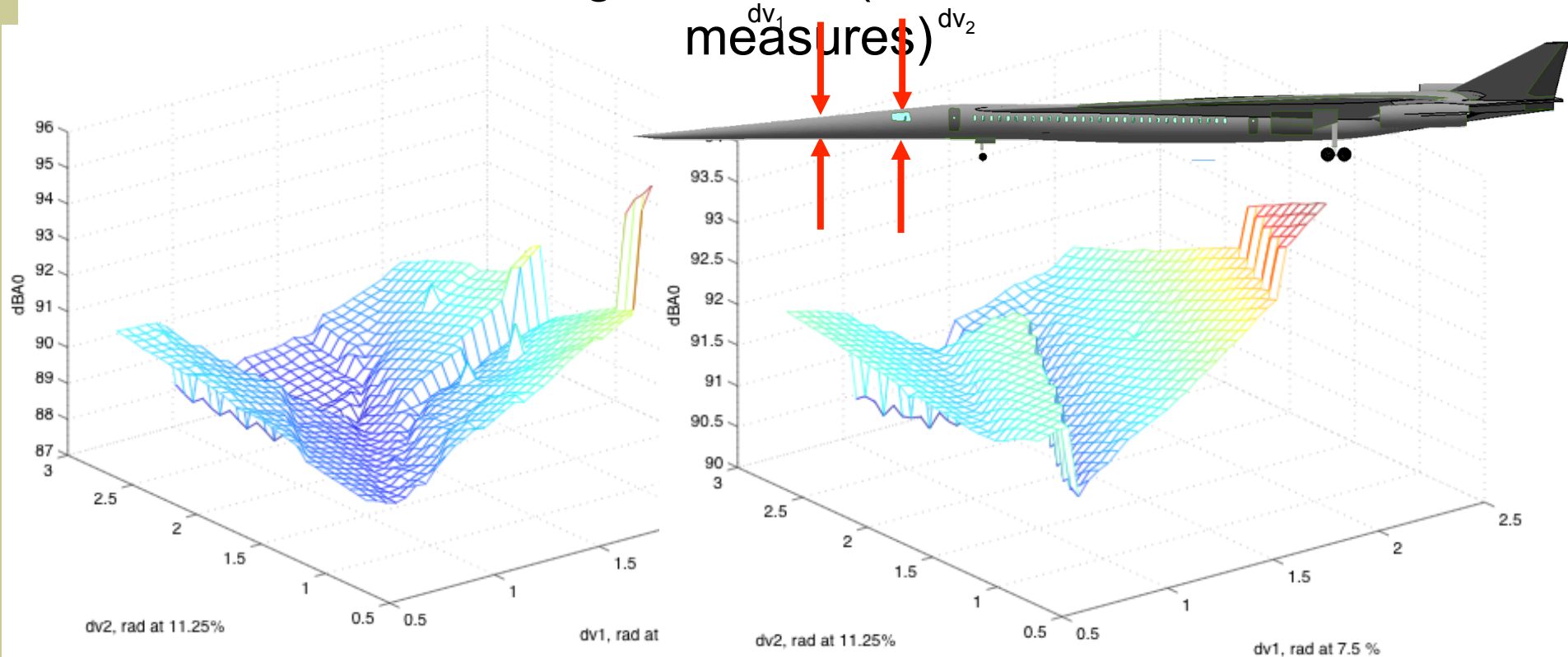
Coefficient of Drag, C_D , vs. radii of two fuselage stations





Why Is Low-Boom Design Difficult? (2)

Ground boom loudness vs. radii of two fuselage stations (two different measures)

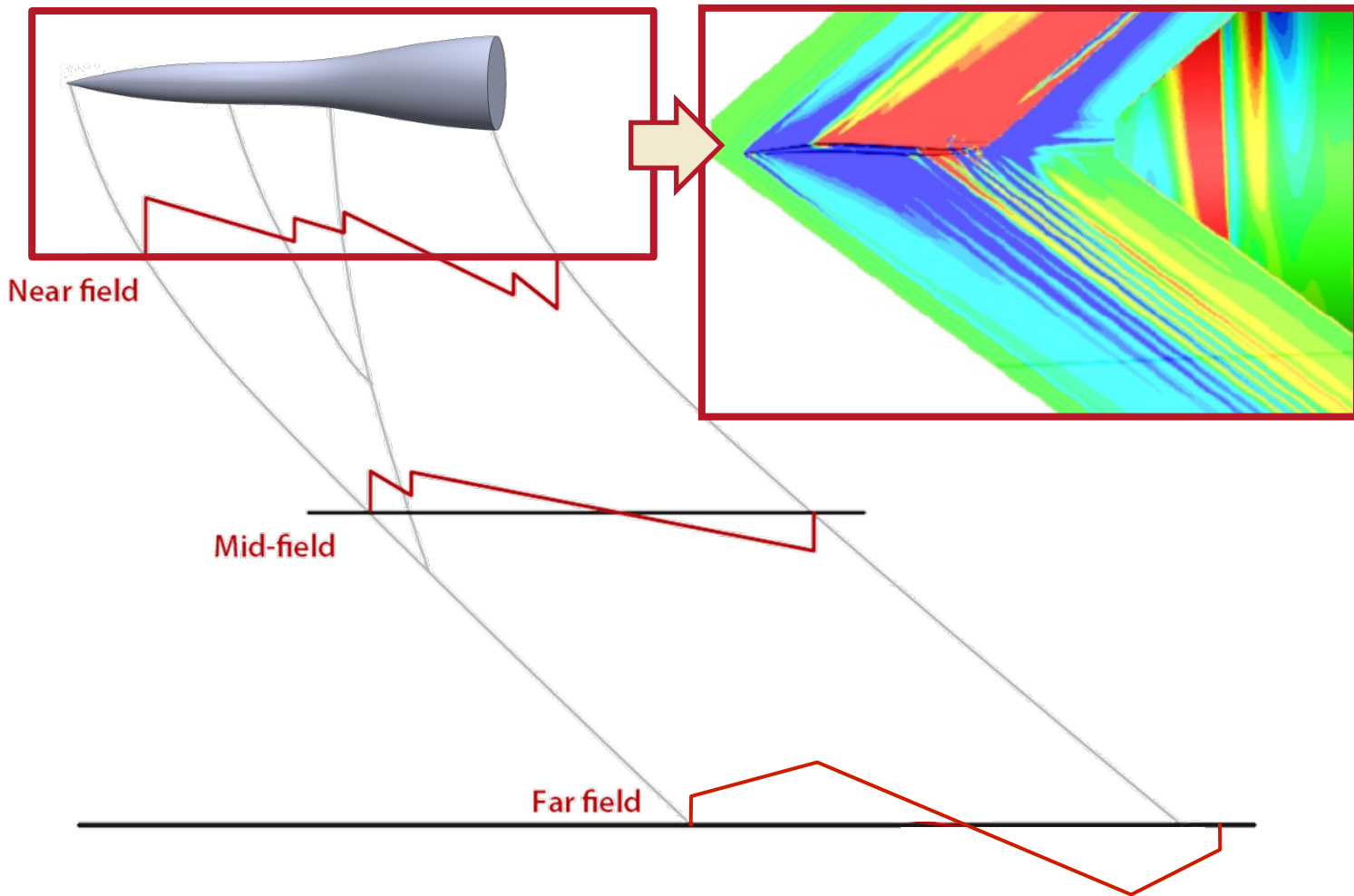




Outline

- The challenge of low-boom design
- **Regularizing the design process**
- N+2 vehicle design efforts
- Low-Boom Flight Demonstrator ongoing efforts
- Conclusions & future work

Regularization: Equivalent Area Distributions



- **CFD-based equivalent area inverse design**
Note that multiple $A_e(x;\theta)$ need to be accounted for



N+2 Supersonic Passenger Jet Concept



Cruise:

Ma 1.6-1.8

Sonic Boom:

65-70 PLdB

Fuel Efficiency:

baseline + 15%

Range:

4000 nmi

Payload:

35-70 pax

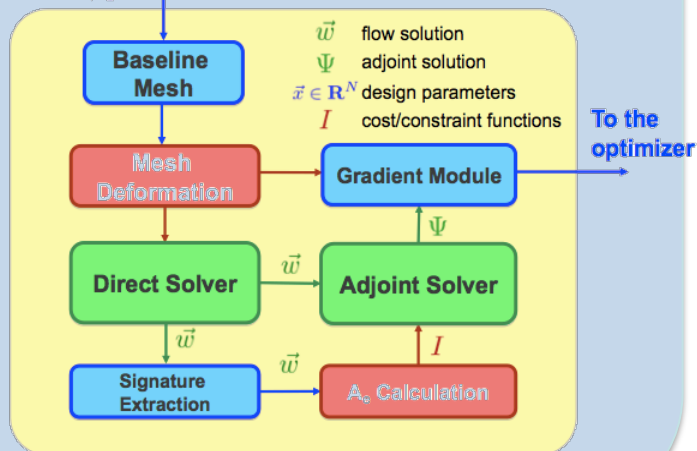
- **Reduce Boom Noise, Reduce Drag, Maintain Lift, Structure, Propulsion Integration**

Fully-Parallel Shape Optimization Tools

Direct connection to gradient-based optimization

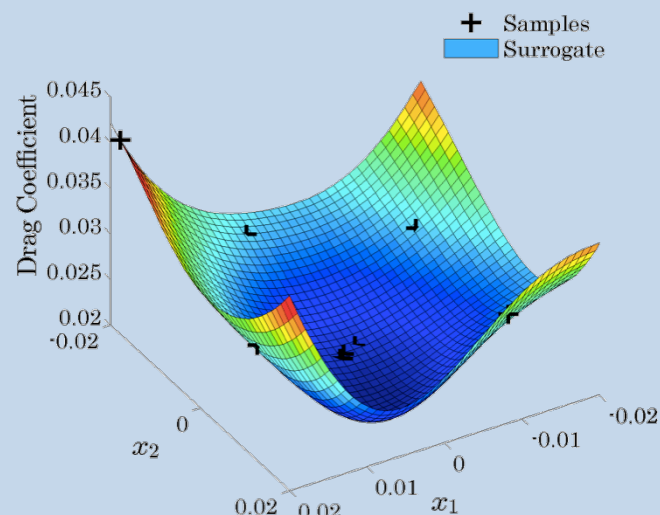
From the optimizer

$\vec{x} \in \mathbb{R}^N$



Gradient-Enhanced GPR
Surrogate Models for Optimization

Objective Surface



Direct solver, adjoint solver, mesh deformation, grid adaptation, fluid/structure simulation, python wrappers...and much more
Under active development by the Aerospace Design Lab

<http://su2.stanford.edu>

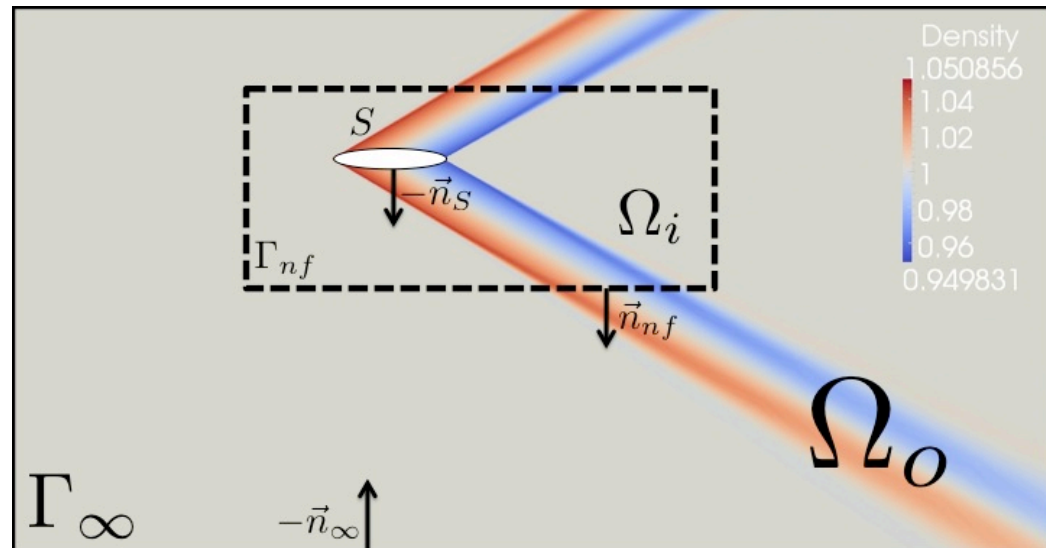
SU² Ver. 3.2 will be released during the Aviation 2014 Conference, 10,000+ downloads to date (May 2014)

Analysis / sensitivity procedure

Surface sensitivities using adjoint methods

The fluid domain is typically bounded by a disconnected boundary that is divided into a “far-field” component, and a solid wall boundary.

We **further subdivide the fluid domain into two sub-domains** separated by a “near-field” boundary.



We are interested in **sensitivities of cost functions** of the kind

$$J = \int_S \vec{d} \cdot (P \vec{n}_S) ds + \int_{\Gamma_{nf}} g(x, P) ds = \int_S j_S ds + \int_{\Gamma_{nf}} j_{nf} ds,$$

where P is the value of the static pressure, and \vec{d} is an arbitrary constant vector to be defined later on.

S. K. Nadarajah, J. J. Alonso, and A. Jameson, “Sonic Boom Reduction using an Adjoint Method for Wing-Body Configurations in Supersonic Flow”, AIAA Paper 2002-5547, 9th AIAA/ISSMO Symposium on Multidisciplinary Analysis and Optimization Conference, September 4-6, 2002, Atlanta, GA.

Analysis / sensitivity procedure

Surface sensitivities using adjoint methods

The last step is to subtract the previous equations to obtain the complete variation of the functional

$$\begin{aligned} \delta J = & \int_S (\vec{d} \cdot \vec{n}_S) \delta P \, ds - \int_S (\vec{n}_S \cdot \vec{\varphi}) \delta P \, ds + \int_{\Gamma_{nf}} \frac{\partial g(x, P)}{\partial P} \delta P \, ds \\ & - \int_{\Gamma_{nf}} \Delta \Psi \left(\vec{n}_{nf} \vec{A} \right) \delta U \, ds + \int_S \left(\vec{d} \cdot \vec{\nabla} P + (\partial_n \vec{v} \cdot \vec{n}_S) \vartheta + \nabla_S(\vec{v} \vartheta) \right) \delta S \, ds. \end{aligned}$$

And solving the adjoint equations subject to **appropriate boundary conditions**

$$\begin{cases} \vec{n}_S \cdot \vec{\varphi} = \vec{d} \cdot \vec{n}_S \\ \vec{\nabla} \Psi \left(\vec{n}_{nf} \cdot \vec{A} \right) = \frac{\partial g(x, P)}{\partial P} = h(x, P), \end{cases}$$

to obtain the **sensitivity of the cost function with respect to the motion of each and every point on the surface of the mesh** = surface shape sensitivities

$$\delta J = \int_S \left(\vec{d} \cdot \vec{\nabla} P + (\partial_n \vec{v} \cdot \vec{n}_S) \vartheta + \nabla_s(\vec{v} \vartheta) \right) \delta S \, ds = \int_S \frac{\partial J}{\partial S} \delta S \, ds.$$



Adj. formulation using equiv. area

Equivalent area adjoint derivation

The equivalent area is the Abel transform of the NF pressure distribution

$$A_e(x; \theta) = \int_0^x C(P - P_\infty)(x - t)^{1/2} dt,$$

We are interested in the L-2 norm of the difference between the area and a target:

$$J = \sum_{i=0}^{N-1} \omega_i [A_e(x_i) - A_t(x_i)]^2$$

A variation in this cost function can be written as

$$\delta J = \sum_{i=0}^{N-1} 2\omega_i [A_e(x_i) - A_t(x_i)] \delta A_e(x_i).$$

using the short-hand notation $\delta A_e(x) = \int_0^x C(x - t)^{1/2} \delta P dt.$

The key question is: **can we handle this kind of cost function using the methodology described earlier?**



Adj. formulation using equiv. area

Equivalent area adjoint derivation

Fortunately, **the answer is YES**. With some algebra...

$$\delta J = \sum_{i=0}^{N-1} \left[2\omega_i [A_e(x_i) - A_t(x_i)] \sum_{j=0}^{i-1} \int_{x_j}^{x_{j+1}} C(x_i - x)^{1/2} \delta P dx \right],$$

where $\Delta A_e(x_i) = 2\omega_i [A_e(x_i) - A_t(x_i)] C$.

And the variation of the objective function can be written as

$$\delta J = \sum_{j=0}^{N-2} \int_{x_j}^{x_{j+1}} \sum_{i=j+1}^{N-1} \left(\Delta A_e(x_i) (x_i - x)^{1/2} \right) \delta P dx.$$

The adjoint boundary conditions that eliminate the dependence on the fluid flow variation in the inverse equiv. area shape design problem is:

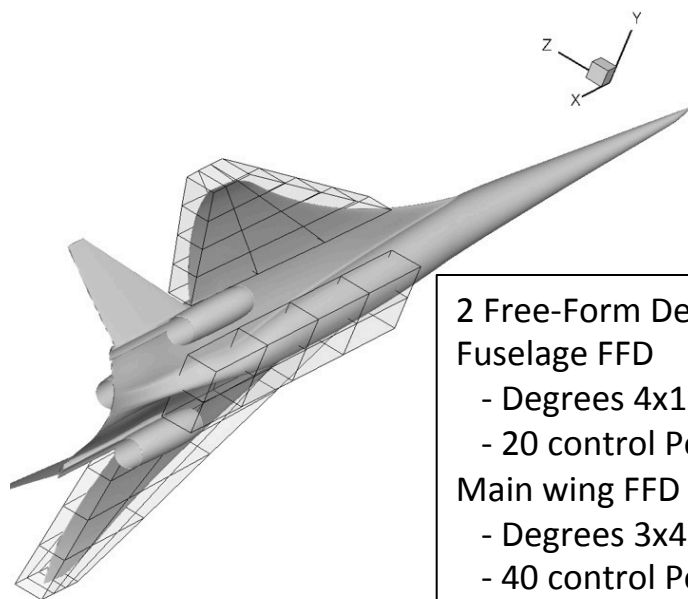
$$\vec{\nabla} \Psi \left(\vec{n}_{nf} \cdot \vec{A} \right) = h(x, P)$$

where

$$h(x, P) = \begin{cases} 0 & , \text{ if } -L < x < x_0, \\ \sum_{i=j+1}^{N-1} \Delta A_e(x_i) (x_i - x)^{1/2} & , \text{ if } x_0 \leq x \leq x_{N-1}, \\ 0 & , \text{ if } x_{N-1} < x < L, \end{cases}$$



A_e Design Using Multiple Azimuthal Angles



2 Free-Form Def. boxes:
Fuselage FFD

- Degrees 4x1x1
- 20 control Points

Main wing FFD

- Degrees 3x4x1
- 40 control Points

Geometry: 1043

Cells: 4,819,934. Nodes: 1,192,791

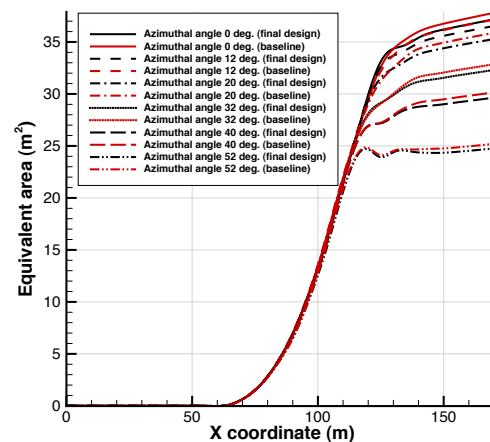
Mach number: 1.7. Angle of attack: 2.1

Free-stream pressure: 15,473.81 Pa

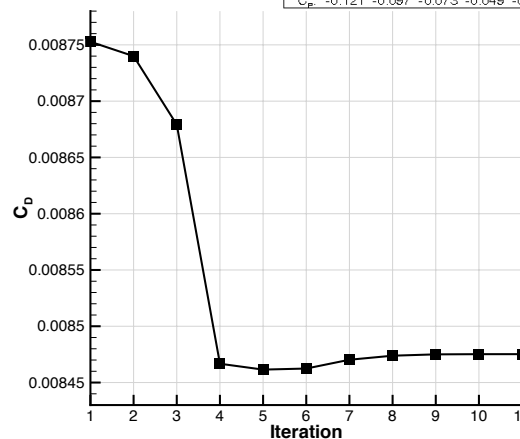
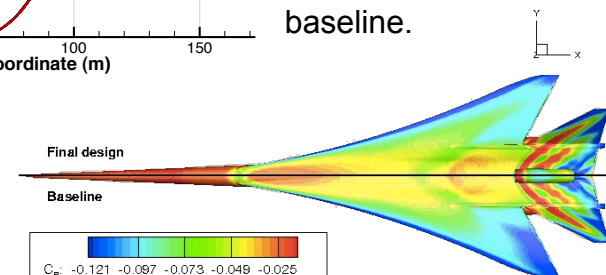
Free-stream temperature: 216.65 K

Multi-objective minimization problem with constraints (min C_L , min C_{My}).

$$OF = \alpha C_D + (1.0 - \alpha) \sum_{\phi=0^\circ}^{\phi=60^\circ} (EA - EA_{baseline})^2$$



~1.5% max difference between Final Design Equivalent Area and the baseline.



2.1% Objective Function reduction.
3.2% C_D reduction.



Outline

- The challenge of low-boom design
- Regularizing the design process
- **N+2 vehicle design efforts**
- Low-Boom Flight Demonstrator ongoing efforts
- Conclusions & future work

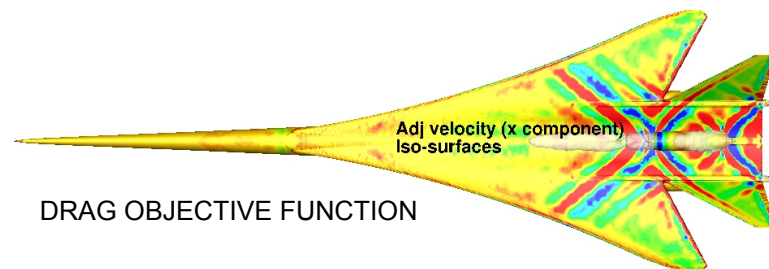
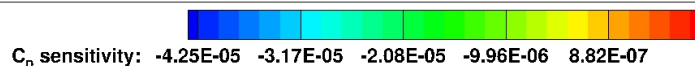
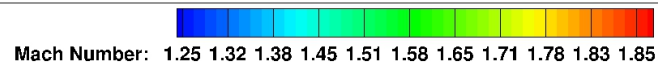
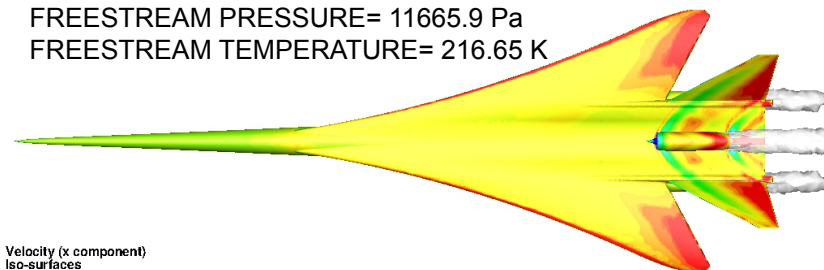
Direct and Adjoint Simulations with Engines

MACH NUMBER= 1.7

AoA= 2.1

FREESTREAM PRESSURE= 11665.9 Pa

FREESTREAM TEMPERATURE= 216.65 K

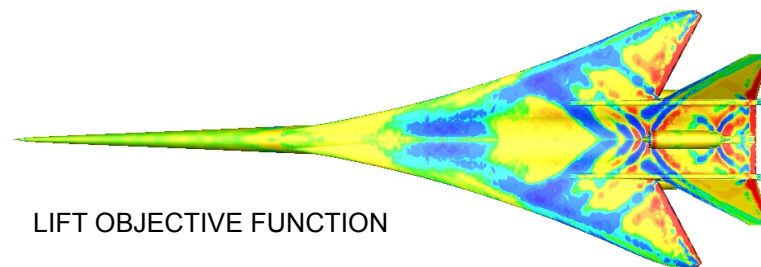
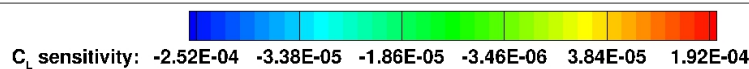
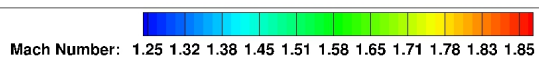
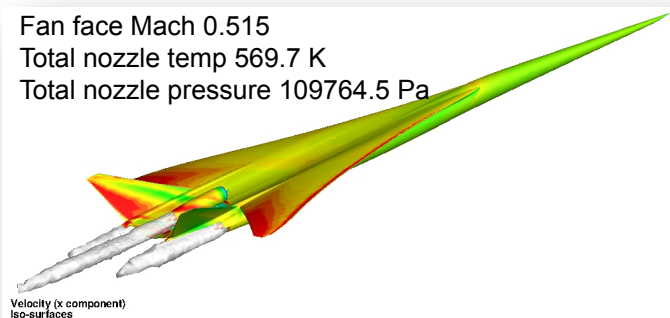


DRAG OBJECTIVE FUNCTION

Fan face Mach 0.515

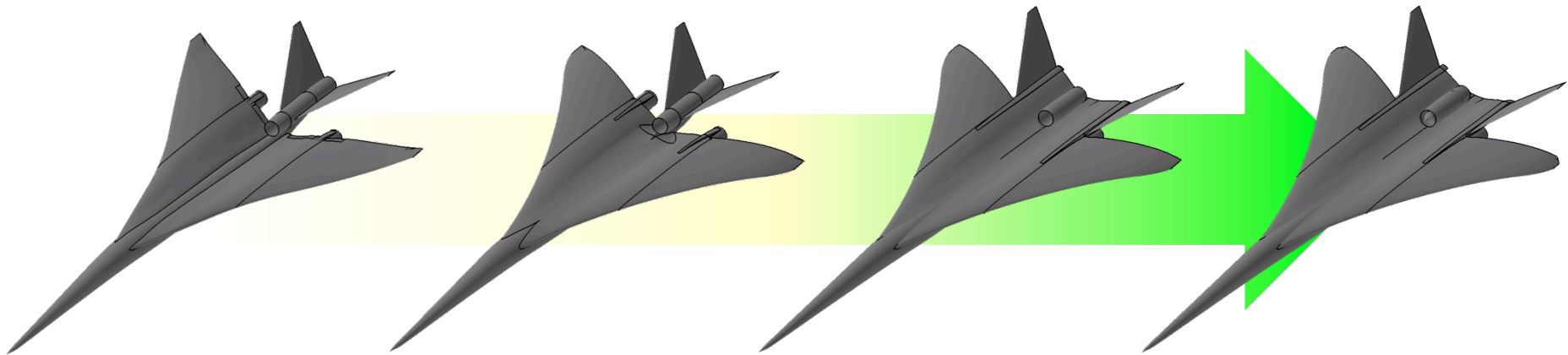
Total nozzle temp 569.7 K

Total nozzle pressure 109764.5 Pa



LIFT OBJECTIVE FUNCTION

Configuration Evolution



Configuration 1021
Phase I tri-jet



LM3

Configuration 1040
Refined tri-jet

Configuration 1043
Aft-deck



LM4 and LTWT

Configuration 1044
Aft-deck w/ prop effects

Configuration 1044-2
Stanford mod

Configuration 1044-3b
Unanalyzed mod rollup

Configuration 1044-x
Phase II going-fwd

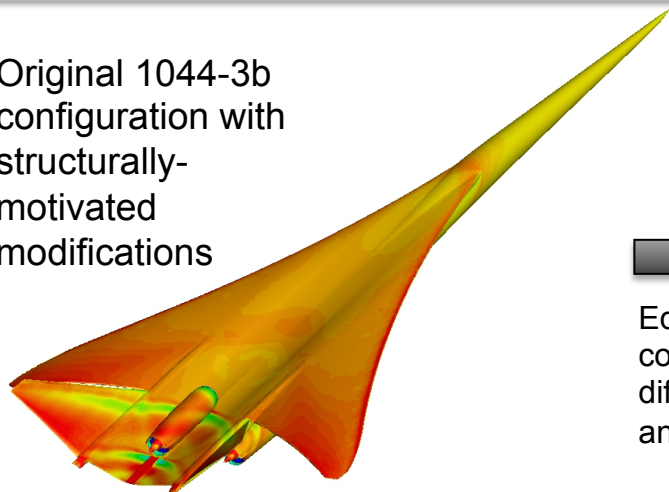
Configuration Evolved Significantly During Phase 2 Effort



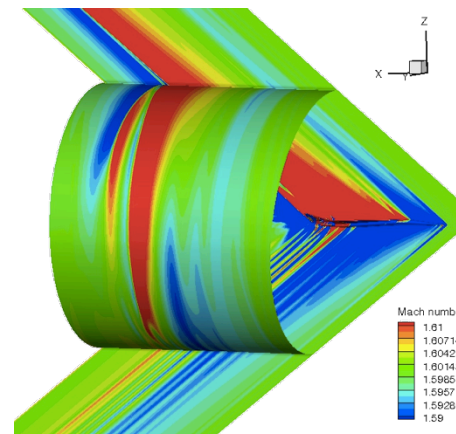
Recovering 1044-1 Ae Starting from 1044-3b

It is possible to recover the boom performance after including the structurally-motivated and engine modifications to the baseline aerodynamic shape?

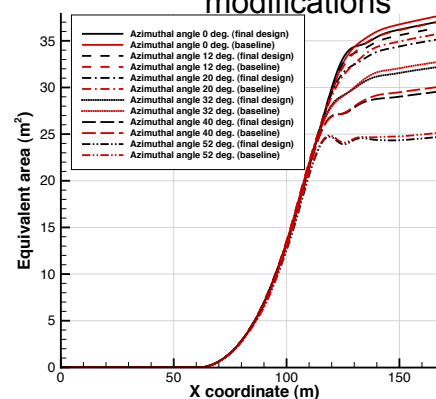
Original 1044-3b configuration with structurally-motivated modifications



Equivalent area computation at different azimuthal angles



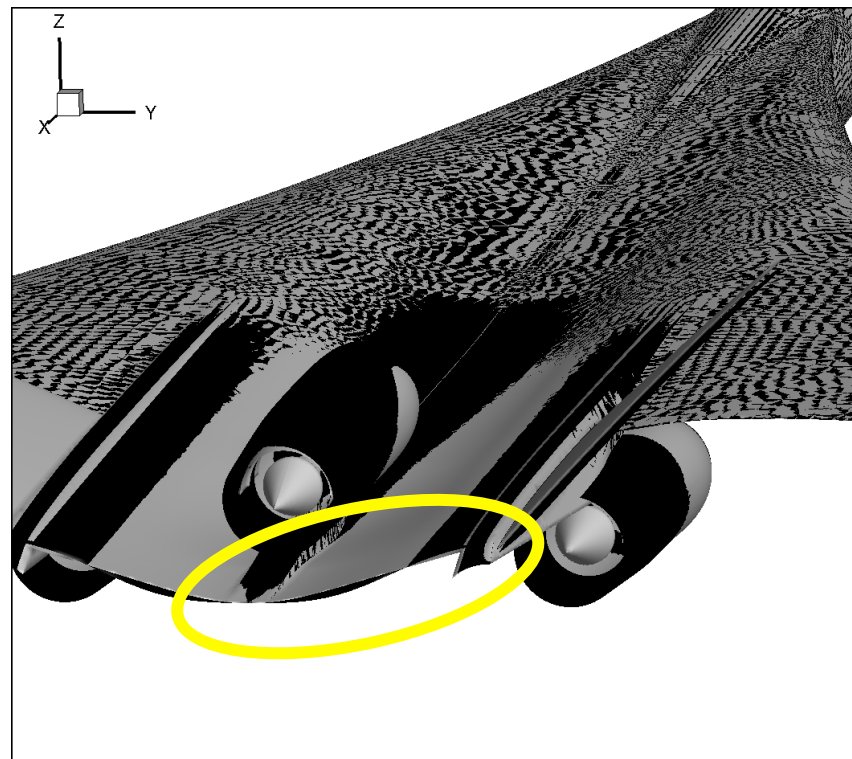
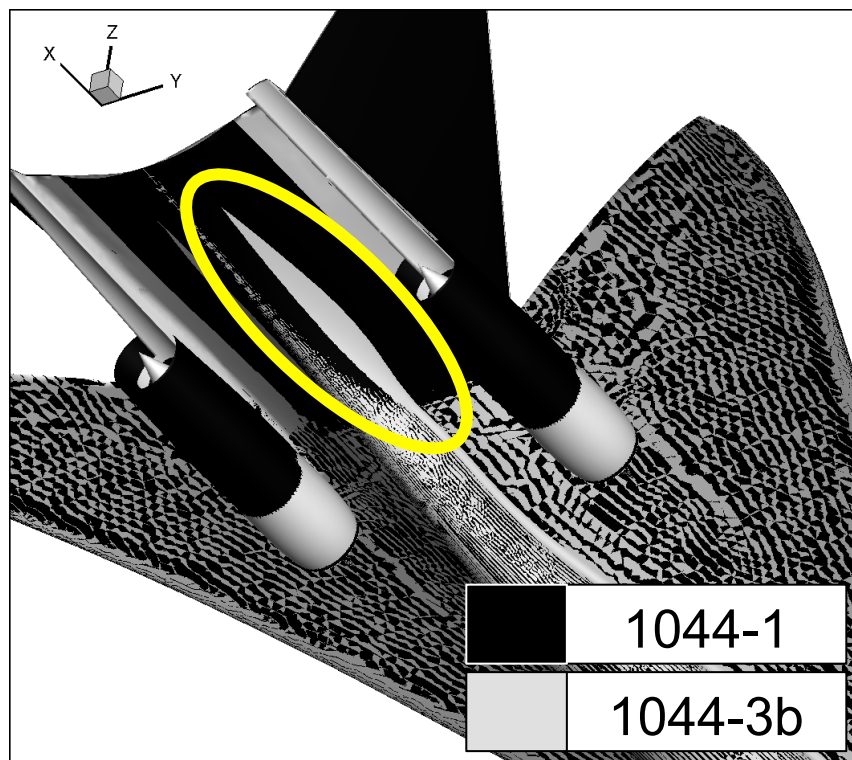
Comparison with baseline 1044-1 configuration without structurally-motivated modifications



Optimization to Recover Equivalent Area with CL, CD, and CM constraints.



Comparison of 1044-1 and 1044-3b



- LM 1044-3b was modified to take advantage of better wing-body blending, and improved load paths through aft strut
- Engine nacelle/nozzle design also updated based on work by GE



Optimization Problem Description

Min. $J(\mathbf{x})$

$\mathbf{x} \in \mathbb{R}^N$

s.t. $C_L(\mathbf{x}) > 0.136$

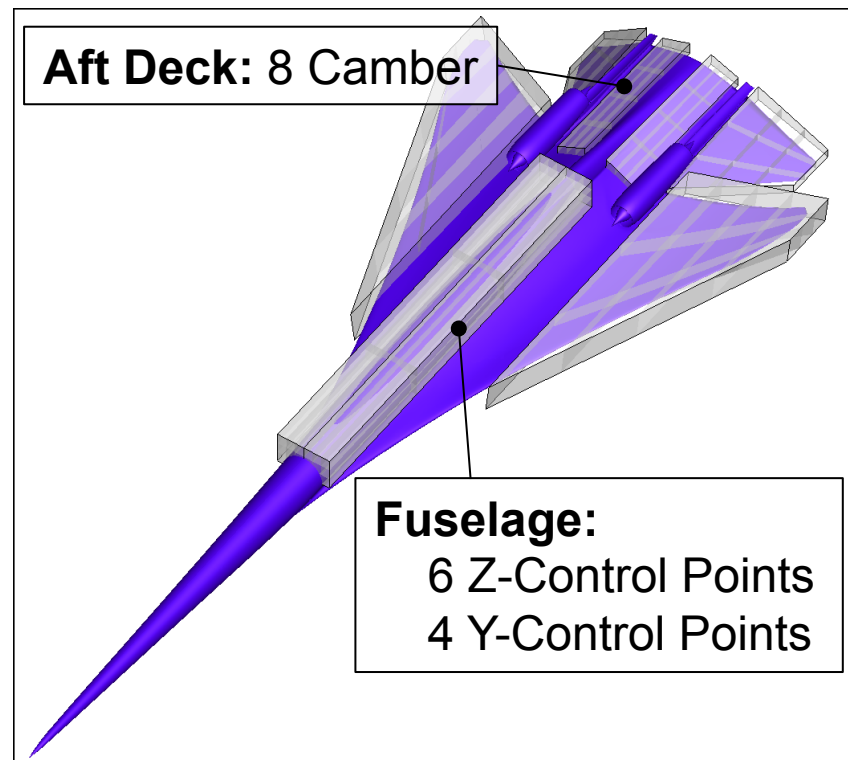
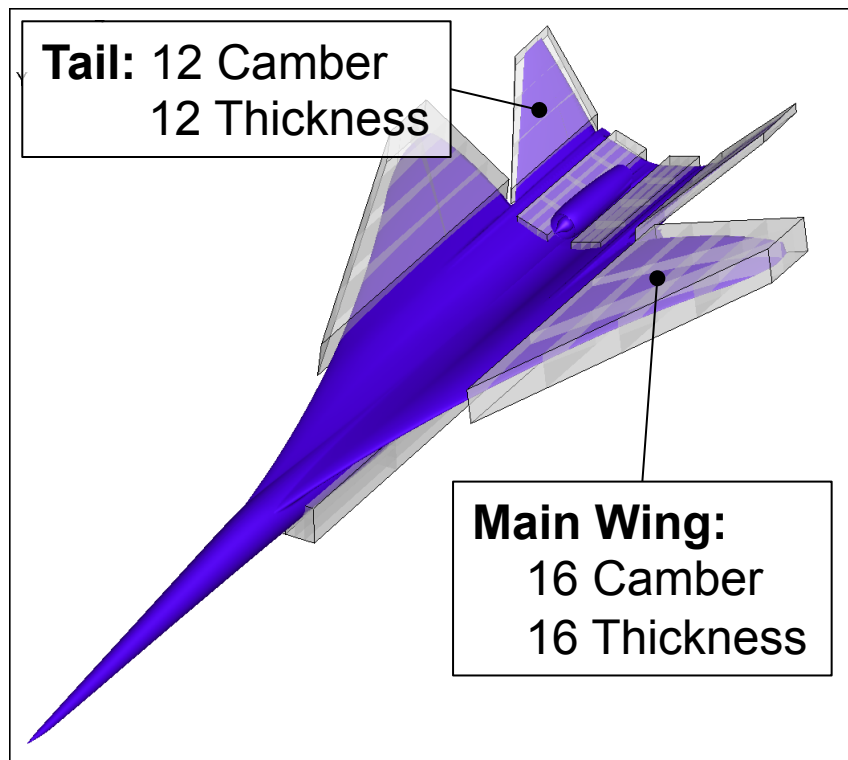
- $Ma = 1.7$, $AoA = 2.1^\circ$,
 $H = 50,000$ ft
- Recover 1044-1 target
equivalent area distribution
- Near-field at 2 body lengths
- Maintain minimum lift
- Free-Form Deformation (FFD)
design variables

$$J = \sum_{k=0}^M \sum_{i=0}^{N-1} \omega_{ik} [A_e(x_i, \theta_k) - A_t(x_i, \theta_k)]^2$$

- Multiple azimuth formulation maintains off-track performance
- Azimuth angle ranges: 0° to 60° , 2° increments



1044-3b Design Parameterization

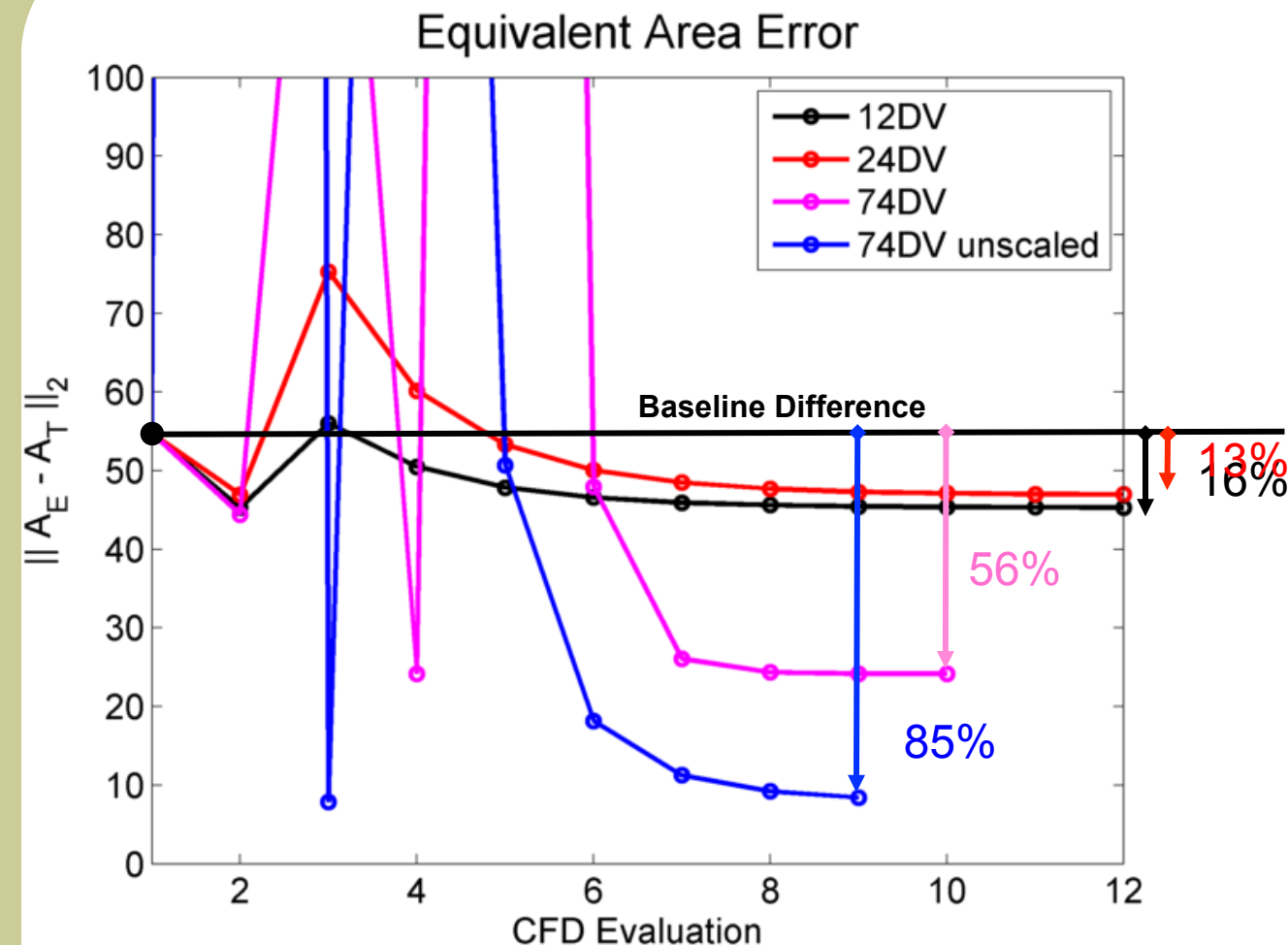


* Mirrored half-body shown

- Total of 74 free-form deformation control points available
- Upper/Lower design variable bounds used to avoid non-physical geometry



Optimization History



12DV: Tail

24DV: Tail, Aft Deck

74DV: Tail, Aft Deck, Main Wing, Fuselage, scaled

74DV: Tail, Aft Deck, Main Wing, Fuselage, un-scaled

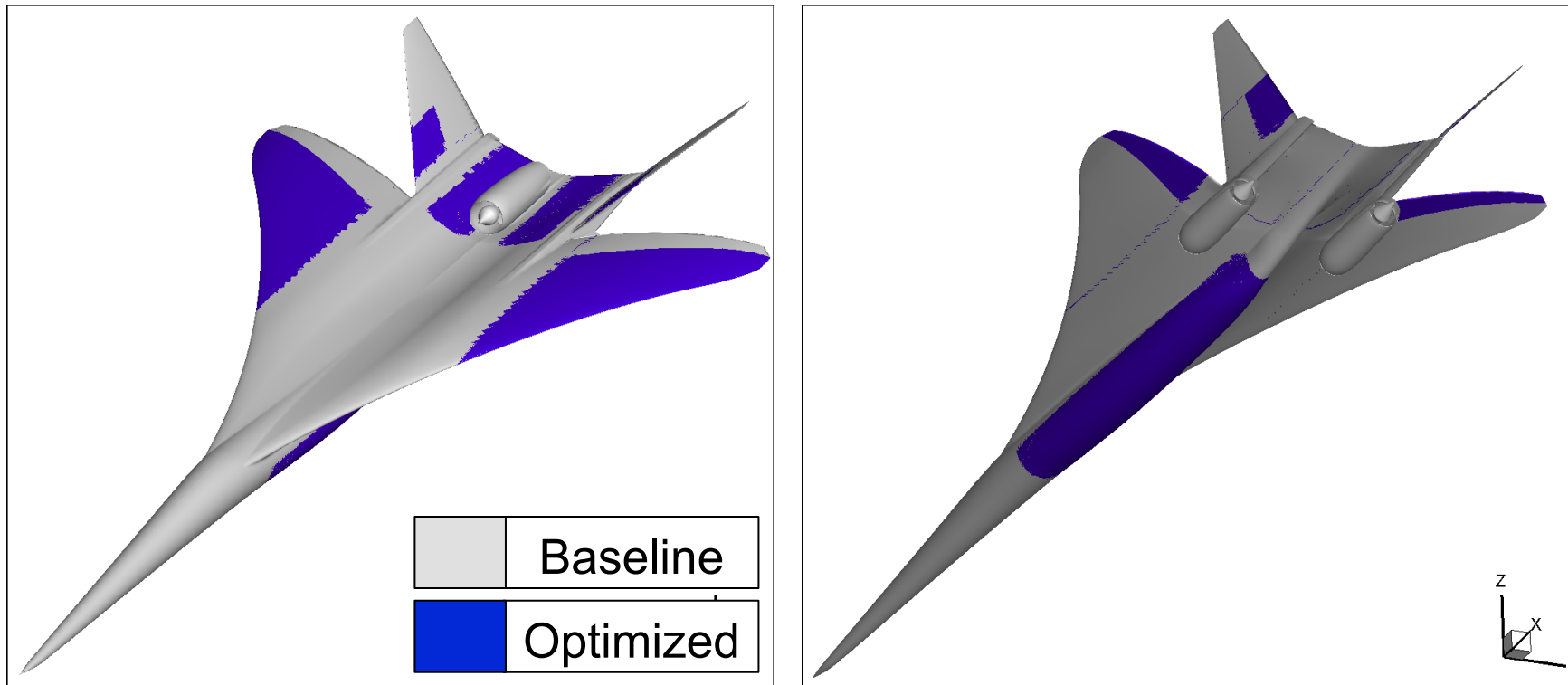
SLSQP Gradient-Based Optimization

Normally objective and constraint data is scaled before given to optimizer

In this study, un-scaled values found larger improvements



Baseline and Optimized Shape (74 DV un-scaled)



- Main wing dihedral increased, trailing edge de-cambered
- Tail angle of attack increased near root
- Fuselage volume increased

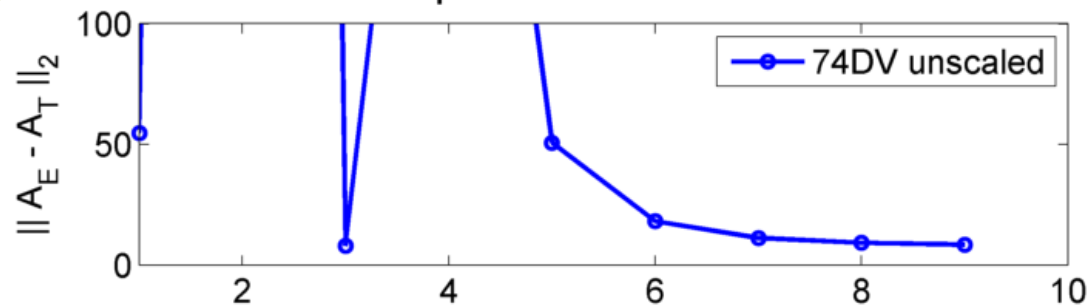


Optimization History

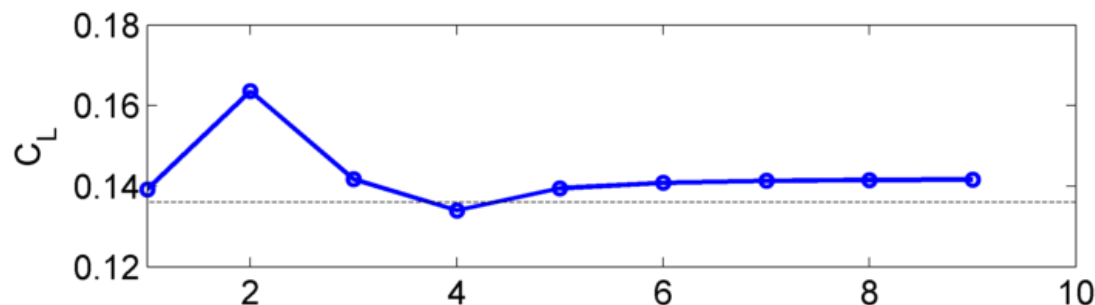
25

$$\frac{\partial C_D}{\partial C_L} = 0.048$$

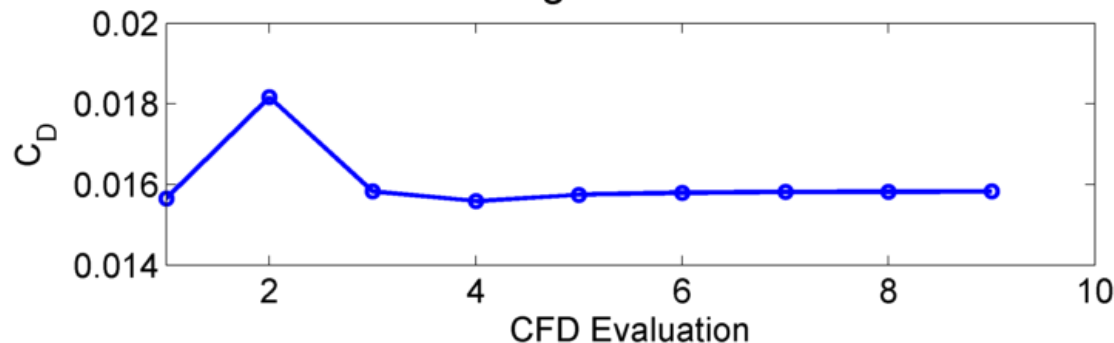
Equivalent Area Error



Lift



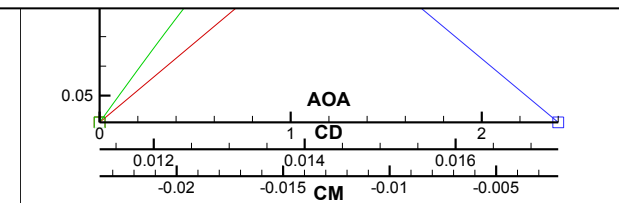
Drag Coefficient



CFD Evaluation



0.8% of difference due to lift increase

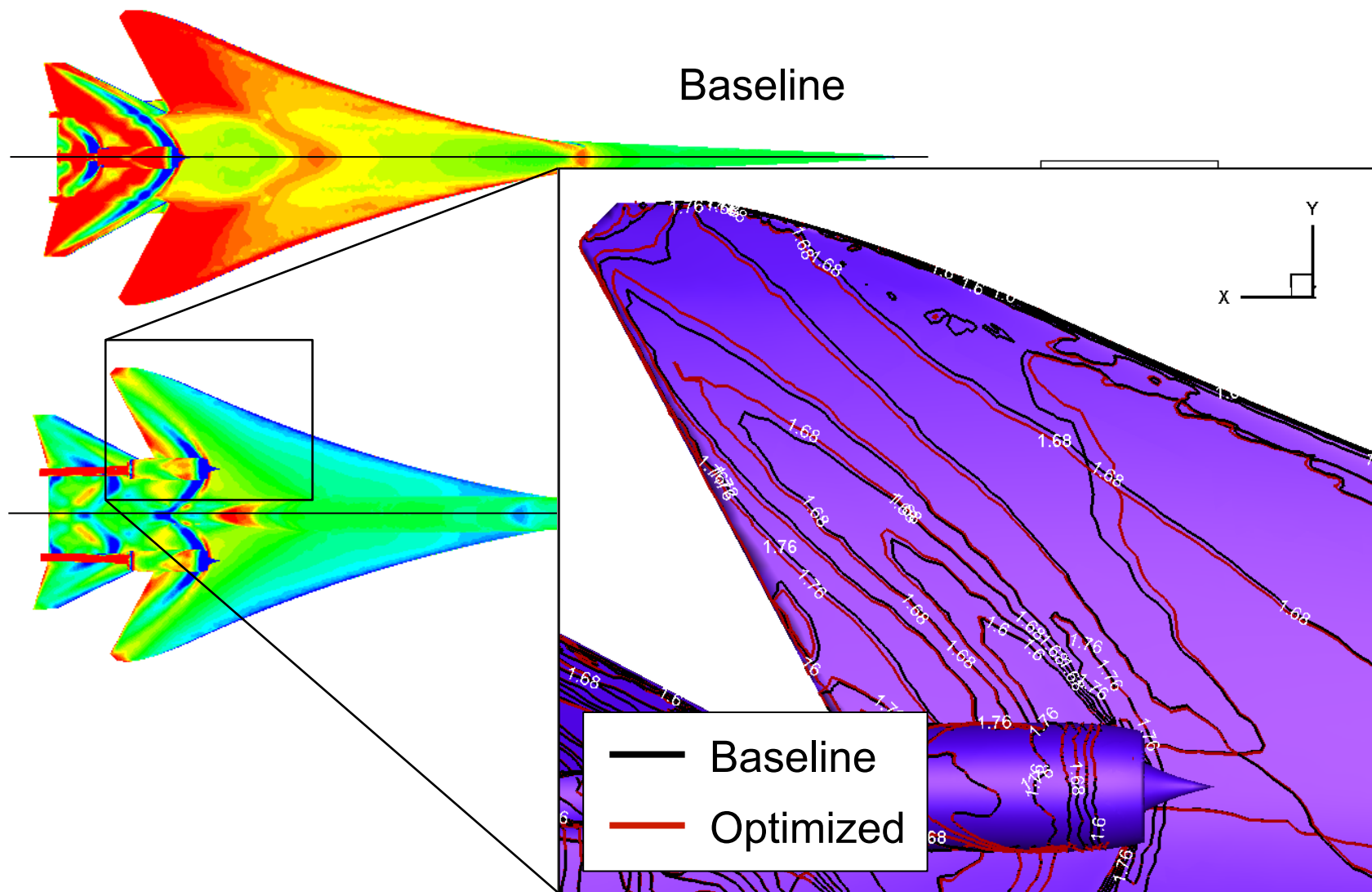


- 85.5% Reduction in Equivalent Area Objective
- +1.8% C_L , +1.1% C_D
- Drag may be minimized by a second optimization with A_e and C_L constraints or an optimization with multiple constraints



Initial and Final Surface Contours

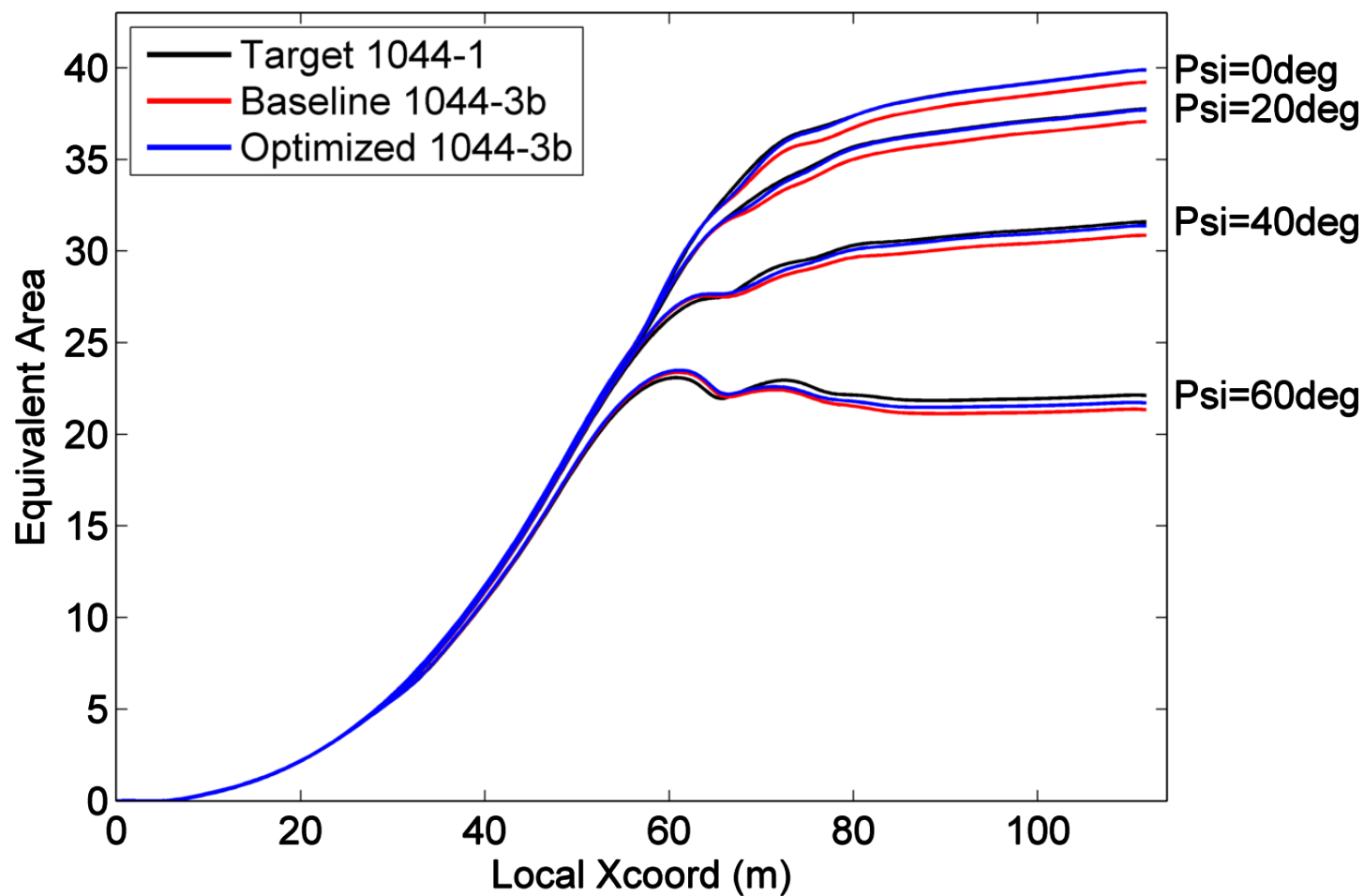
Mach Number





Equivalent Area Distribution Comparison

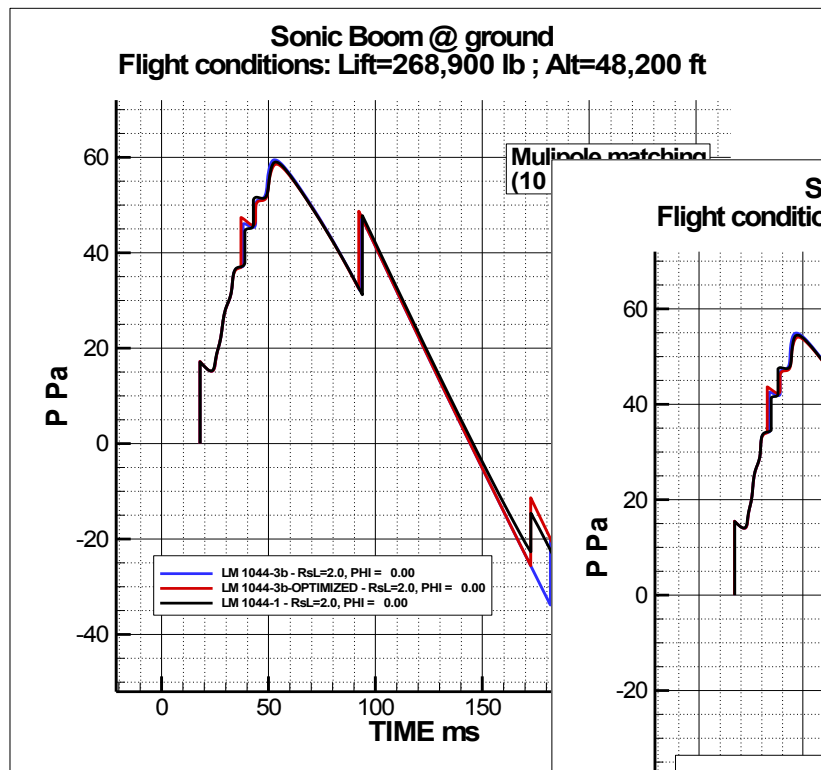
Nearfield Equivalent Area Distributions
Selected Azimuth Angles



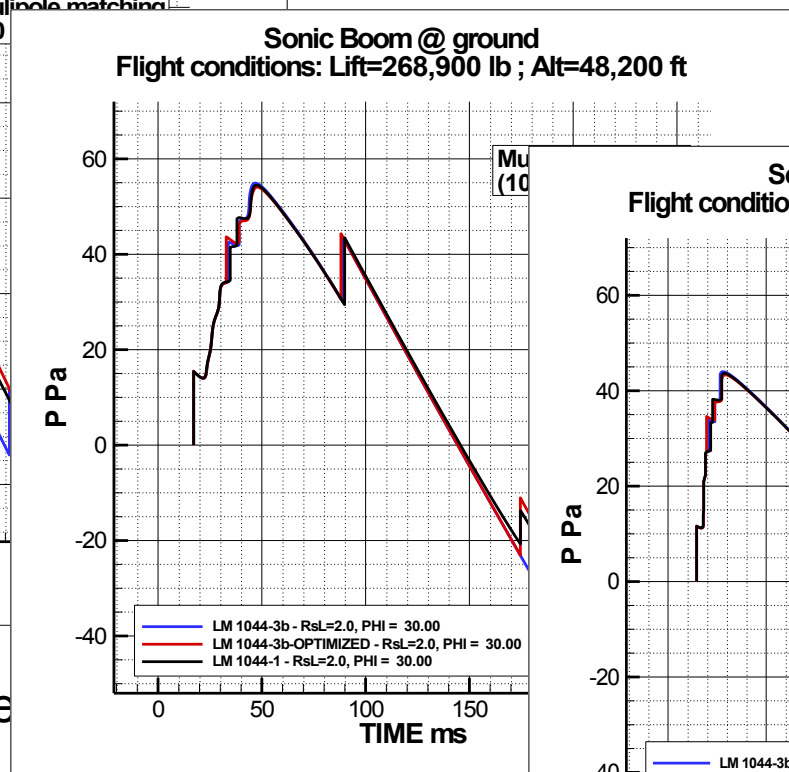


Comparison of Ground Boom signatures

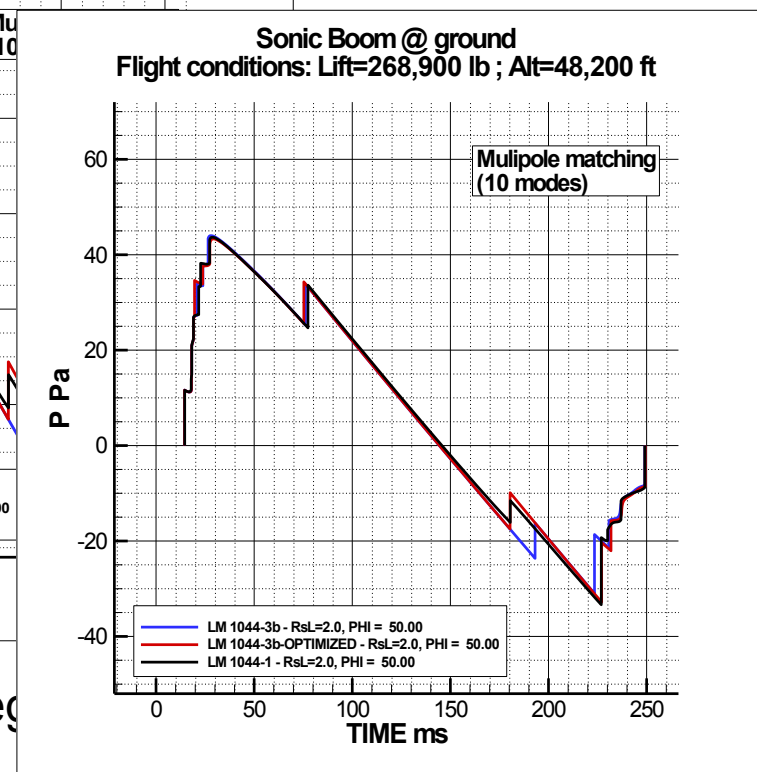
LM 1044-1, -3b and -3b OPTIMIZED configurations



$\Phi = 0$ deg



$\Phi = 30$ deg



$\Phi = 50$ deg



Outline

- The challenge of low-boom design
- Regularizing the design process
- N+2 vehicle design efforts
- Low-Boom Flight Demonstrator ongoing efforts
- **Conclusions & future work**

Conclusions

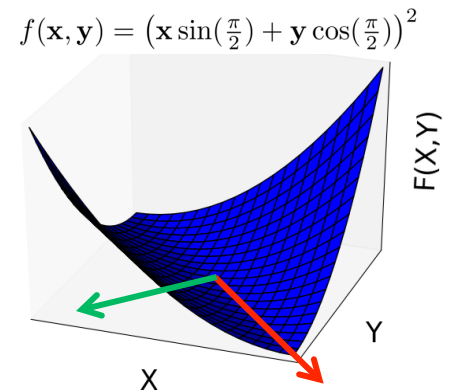
- A number of recent “firsts”
 - Full configuration (75 pax) with a shaped boom signature (front and back; all azimuthal angles)
 - Realizable vehicle (design continues as we speak) to be used as a low-boom flight demonstrator
- Designs enabled by:
 - Advanced CFD and adjoints
 - Better understanding of the design space variations
 - A completely integrated unstructured capability, SU²
- Next steps:
 - Finalize design of LBFD
 - Construct approaches to reduce the size of the design problem



Active Subspace

“A low-dimensional subspace of the inputs that captures global trends of the objective”

- Works by finding eigenvectors of objective **gradients**
- Comparable to Principal Components Analysis
 - PCA: reduce **output** space dimension
 - Active Subspace: reduce **input** space dimension

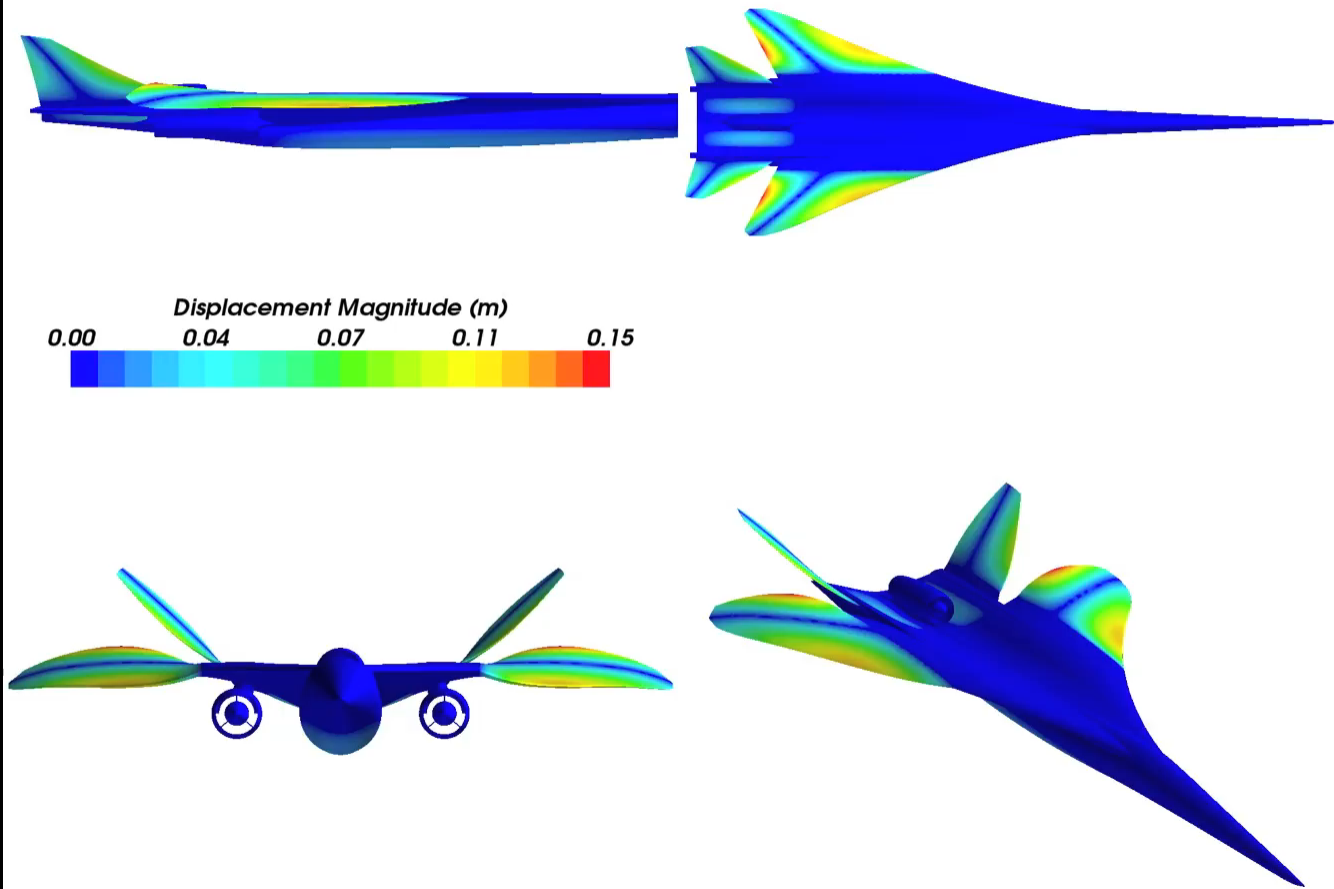


Constantine, P. G., Dow, E., and Wang, Q., “Active subspace methods in theory and practice: applications to kriging surfaces,” 2013.



N+2 Active Subspaces for Lift

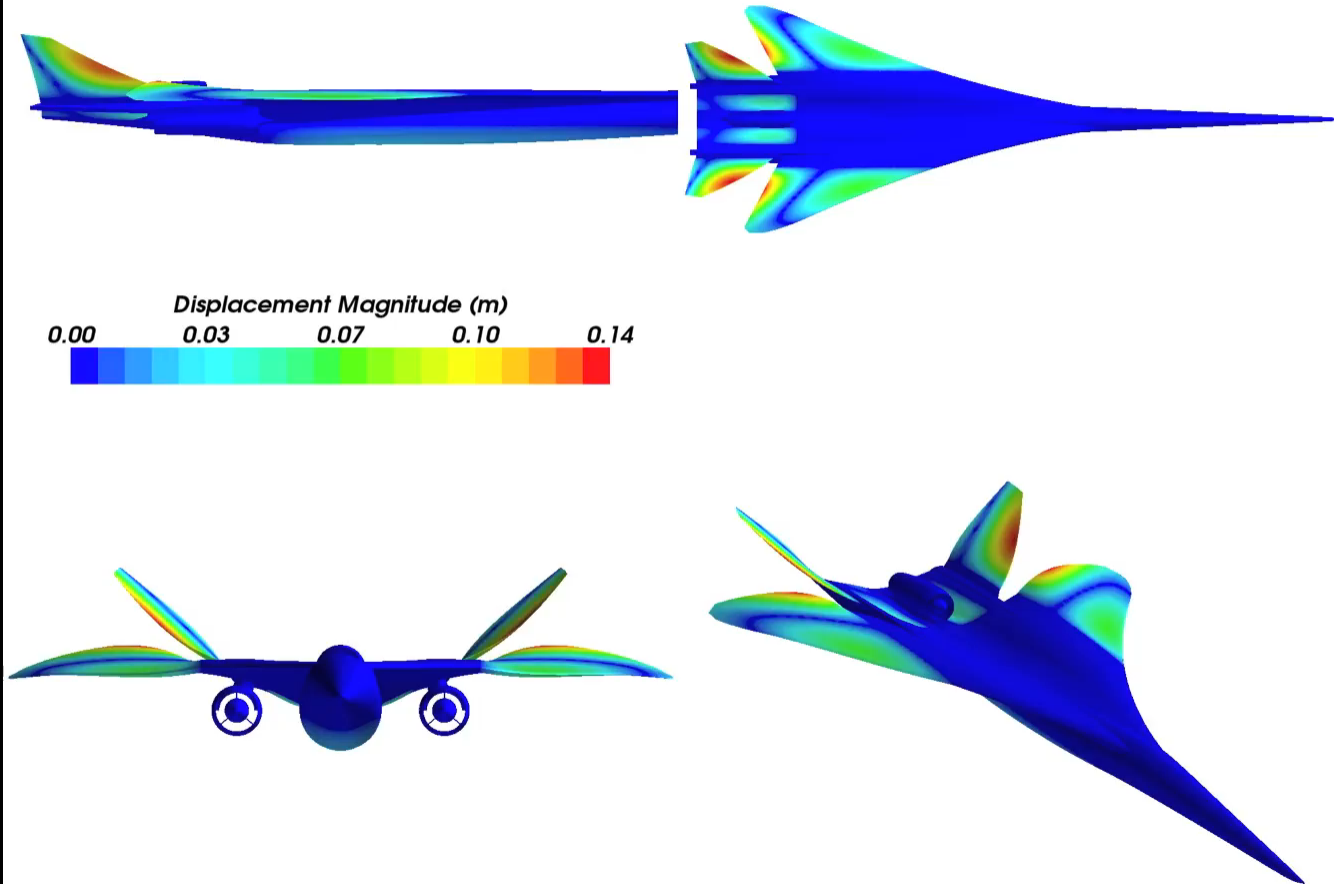
Lift Active Variable 1.





N+2 Active Subspaces for Drag

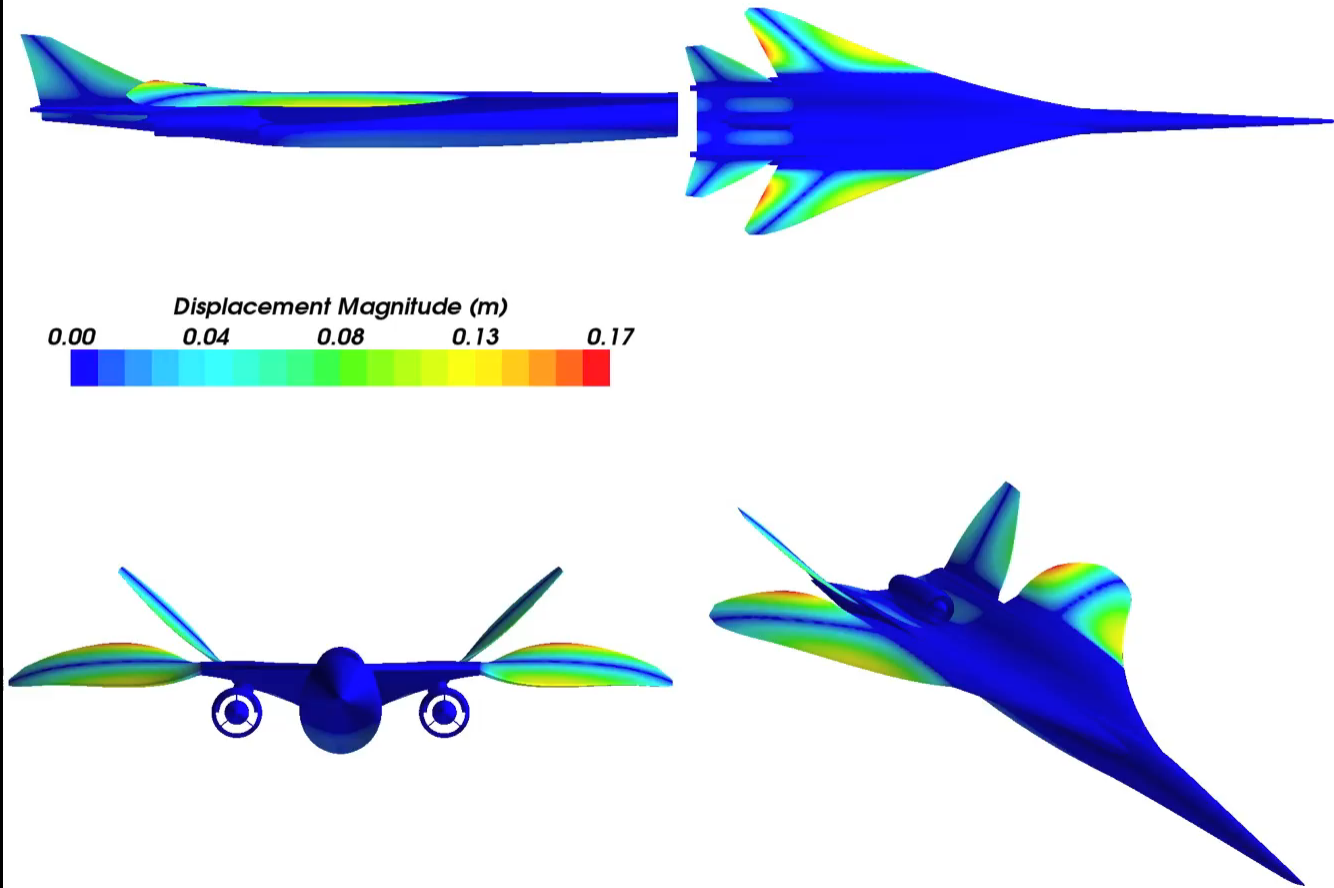
Drag Active Variable 1.





N+2 Active Subspaces for Equiv Area

Equivalent Area Active Variable 1.





The Open-Source CFD Code



aerospacedesignlab

Thanks a lot for your attention!
Questions & Answers

More details in <http://su2.stanford.edu/>